

An “All-in-one” Treatment and Imaging Nanoplatfom for Breast Cancer with Photothermal Nanoparticles

Yuping Fu^{a#}, Hongmei Zhang^{a#}, Jiahui Ye^{b#}, Changrong Chen^d, Yaxuan Yang^b,
Baojuan Wu^b, Xi Yin^b, Jiajun Shi^b, Yun Zhu^e, Cheng Zhao^{c*}, Weijie Zhang^{a,b *}

^a*Division of Breast Surgery, Department of General Surgery, Nanjing Drum Tower Hospital, Nanjing Drum Tower Hospital Clinical College of Traditional Chinese and Western Medicine, Nanjing University of Chinese Medicine, Nanjing, 210008, China*

^b*Division of Breast Surgery, Department of General Surgery, Nanjing Drum Tower Hospital, The Affiliated Hospital of Medical School, Nanjing University, Nanjing, 210008, China*

^c*Department of Gastroenterology, Nanjing Drum Tower Hospital, The Affiliated Hospital of Medical School, Nanjing University, Nanjing, 210008, China*

^d*Division of Emergency Surgery, Department of General Surgery, Nanjing Drum Tower Hospital, The Affiliated Hospital of Medical School, Nanjing University, Nanjing, 210008, China*

^e*Division of Pharmacy Surgery, Department of General Surgery, Nanjing Drum Tower Hospital, The Affiliated Hospital of Medical School, Nanjing University, Nanjing, 210008, China*

[#]Yuping Fu, Hongmei Zhang and Jiahui Ye contributed equally to this manuscript.

Correspondence:

*Cheng Zhao: dg1735099@smail.nju.edu.cn;

*Weijie Zhang: zhangweijie1616@nju.edu.cn.

Supporting information

Sample	Size (nm)	PDI	Zeta potential (mV)
PEG-PCL	135.76 ± 2.47	0.223 ± 0.030	-12.97 ± 0.200
PPSI	158.15 ± 1.73	0.267 ± 0.008	14.66 ± 0.640

Table S1. Comparison of particle size of PEG-PCL and PPSI.

Sample	IR780		PTX		SPIO	
	EE%	LC%	EE%	LC%	EE%	LC%
PEG-PCL	-	-	-	-	-	-
PPSI	16.39	0.82	81.38	4.07	35.99	0.36

Table S2. Comparison of drug loading capacity and encapsulation efficiency of PEG-PCL and PPSI.

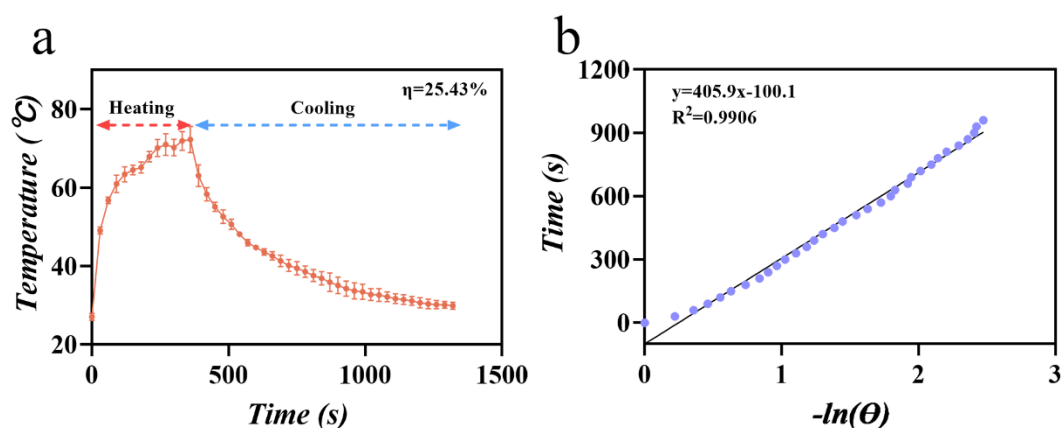


Figure S1. The photothermal conversion effect of PPSI nanoparticles. (a) Temperature changes of PPSI nanoparticles in one heating/cooling cycle. (b) Linear regression curve of temperature cooling time of PPSI nanoparticles.

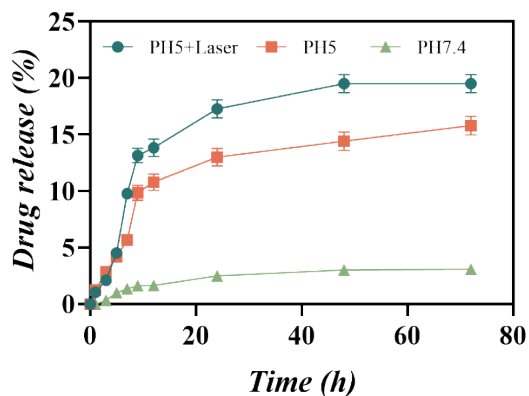


Figure S2. The effects of laser irradiant (808nm, 2W/cm²) and pH on the PTX release rate.

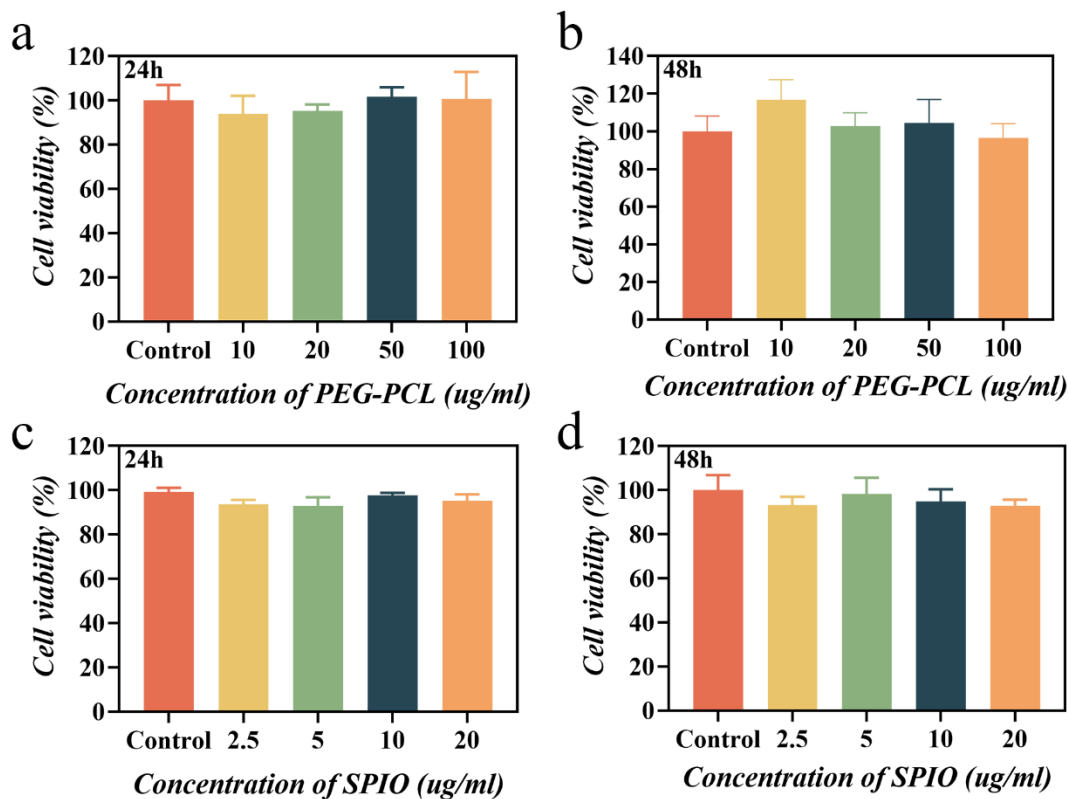


Figure S3. *In vitro* biocompatibility evaluation. (a) Cell viabilities detected by CCK8 assay of 3T3 cells treated with different concentration of PEG-PCL nanoparticles for 24h. (b) Cell viabilities detected by CCK8 assay of 3T3 cells treated with different concentration of PEG-PCL nanoparticles for 48h. (c) Cell viabilities detected by CCK8 assay of 3T3 cells treated with different concentration of PEG-PCL@SPIO

nanoparticles for 24h. **(d)** Cell viabilities detected by CCK8 assay of 3T3 cells treated with different concentration of PEG-PCL@SPIO nanoparticles for 48h.

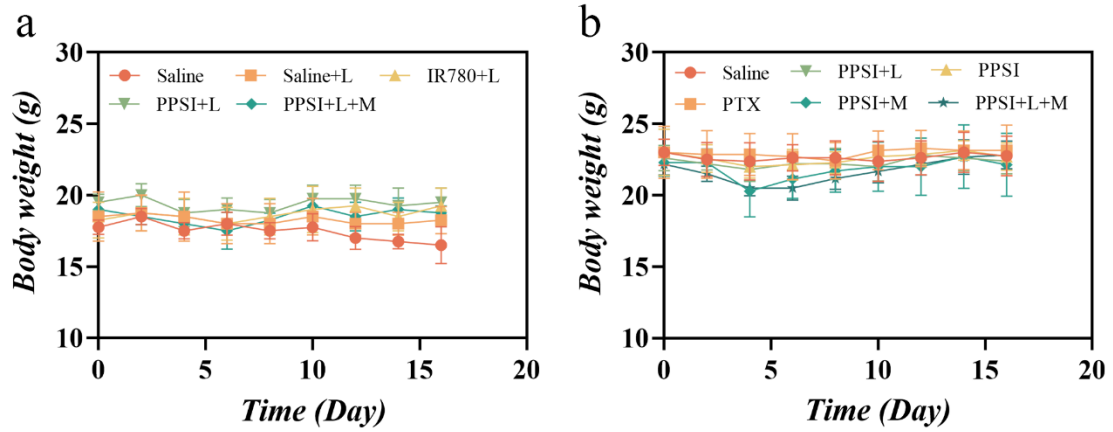


Figure S4. Mean body weights of the mice during the experiment period. **(a)** Changes in body weight in combination therapy versus single photothermal therapy. **(b)** Changes in body weight in combination therapy versus chemotherapy.

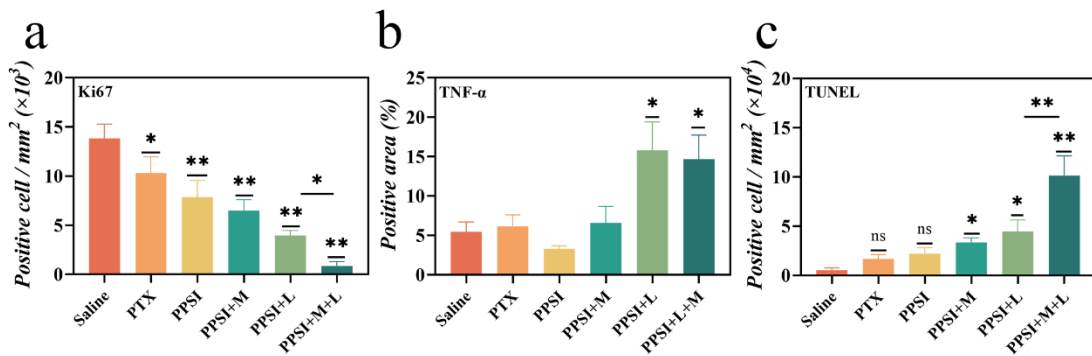


Figure S5. Fluorescence semi-quantitative of Ki-67 and TUNEL and TNF- α in combination therapy versus chemotherapy.

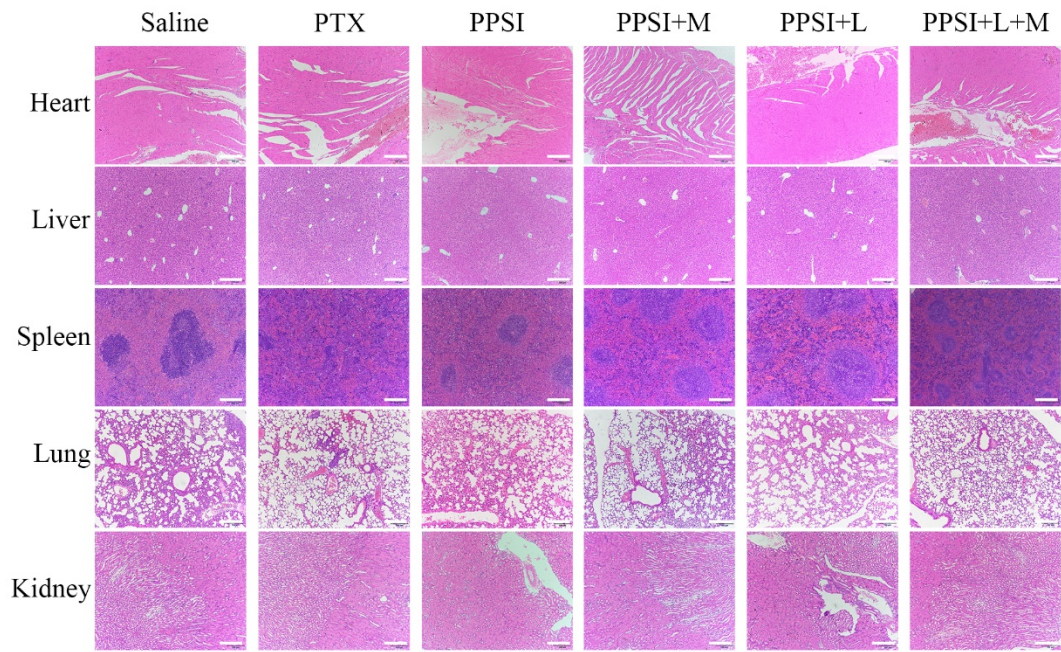


Figure S6. *In vivo* biocompatibility evaluation. HE stained-images of major organs excised at day 16 after treatment. The scale bars are 100 μm .

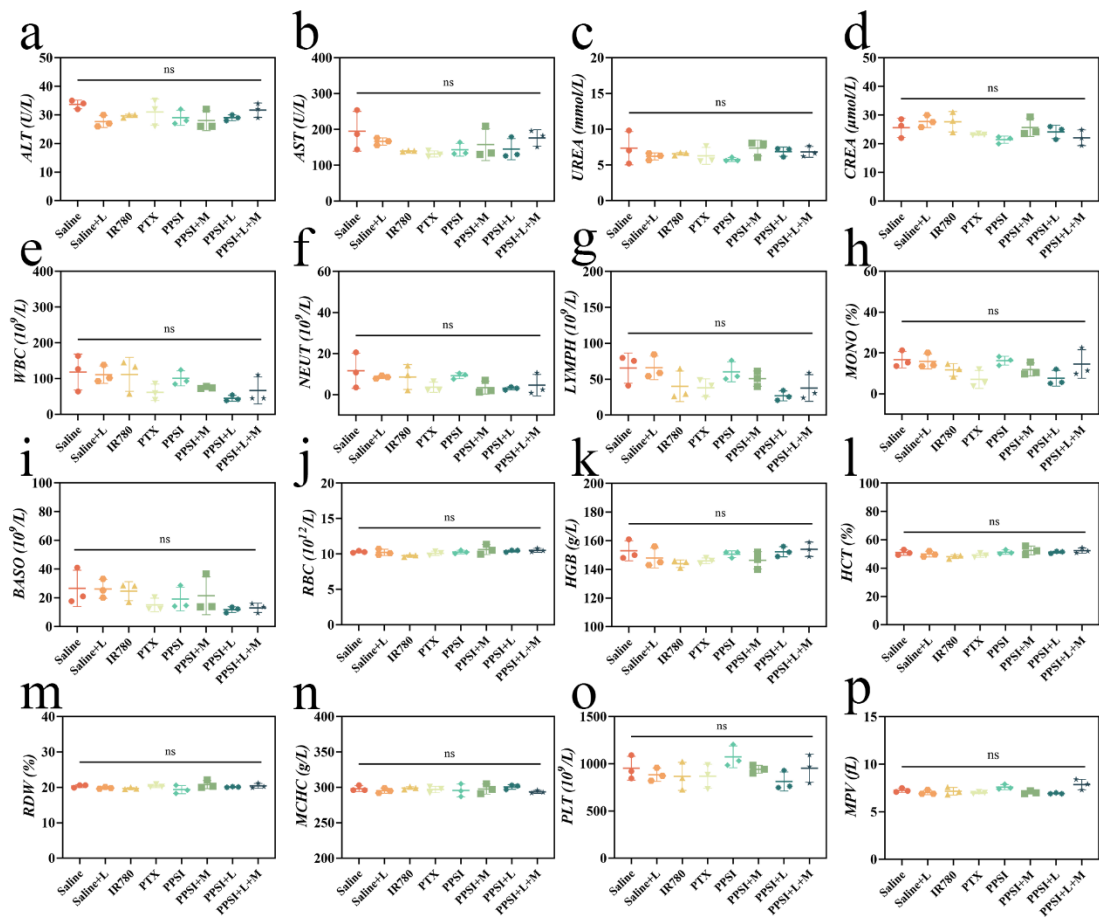


Figure S7. Biochemical indices and blood routine indices in different treatment groups. (a)-(b): liver function indicators. (c)-(d): kidney function indicators. (e)-(i): white blood cell level. (j)-(n): red blood cell and hemoglobin levels. (o)-(p): platelet level.